GLT-1 Transport Stoichiometry Is Constant at Low and High Glutamate Concentrations when Chloride Is Substituted by Gluconate

Anatoli Y. Kabakov*¤, Paul A. Rosenberg*

F. M. Kirby Neurobiology Center and Department of Neurology, Children's Hospital and Harvard Medical School, Boston, Massachusetts, United States of America

¤ Current Address: Biology Department and Volen Center for Complex Systems, Brandeis University, Waltham, Massachusetts, United States of America
* kabakov@brandeis.edu (AYK); paul.rosenberg@childrens.harvard.edu (PAR)

Abstract

Glutamate is the major excitatory neurotransmitter, but prolonged exposure even at micromolar concentrations causes neuronal death. Extracellular glutamate is maintained at nanomolar level by glutamate transporters, which, however, may reverse transport and release glutamate. If and when the reverse occurs depends on glutamate transport stoichiometry (GTS). Previously we found that in the presence of chloride, the coupled GLT-1 glutamate transporter current and its relationship to radiolabeled glutamate flux significantly decreased when extracellular glutamate concentration increased above 0.2 mM, which implies a change in GTS. Such high concentrations are feasible near GLT-1 expressed close to synaptic release site during excitatory neurotransmission. The aim of this study was to determine GLT-1 GTS at both low (19–75 µM) and high (300–1200 µM) glutamate concentration ranges. GTS experiments were conducted in the absence of chloride to avoid contributions by the GLT-1 uncoupled chloride conductance. Mathematical analysis of the transporter thermodynamic equilibrium allowed us to derive equations revealing the number of a particular type of ion transported per elementary charge based on the measurements of the transporter reversal potential. We found that GLT-1a expressed in COS-7 cells co-transports 1.5 Na^+, 0.5 Glu^-, 0.5 H^+ and counter-transports 0.6 K^+ per elementary charge in both glutamate concentration ranges, and at both 37°C and 26°C temperatures. The thermodynamic parameter $Q_{10} = 2.4$ for GLT-1 turnover rate of 19 s^{-1} (37°C, -50 mV) remained constant in the 10 µM–10 mM glutamate concentration range. Importantly, the previously reported decrease in the current/flux ratio at high glutamate concentration was not seen in the absence of chloride in both COS-7 cells and cultured rat neurons. Therefore, only in the absence of chloride, GLT-1 GTS remains constant at all glutamate concentrations. Possible explanations for why apparent GTS might vary in the presence of chloride are discussed.

Introduction

Glutamate is the major excitatory neurotransmitter of the central nervous system, but exposures to even low glutamate concentrations are toxic to neurons [1,2]. The only known clearance mechanism for glutamate is provided by five excitatory amino acid transporters (EAAT1-5) [3]. GLT-1, the rodent analog of human EAAT2, is the major glutamate transporter of the brain. GLT-1 knockout mice die from intractable epilepsy several weeks after birth and have only about 5% of wild-type levels of glutamate uptake activity in cortical synaptosomes [4]. Selective inhibition of GLT-1 by intrahippocampal microinjection of a specific inhibitor (WAY-855, 200–300 nmol) in rat *in vivo* killed the majority of both CA1–4 pyramidal cells and dentate gyrus granule cells [5].

At certain conditions defined by the membrane potential and by transmembrane concentration gradients of the transported ions, glutamate transporters may reverse transport and release glutamate. If and when the reverse occurs depends on glutamate transport stoichiometry (GTS), which ultimately affects neuronal survival. The GTS of glutamate transporters EAAT3, GLT-1 and GLAST has been determined previously as $3Na^+: 1Glu^-: 1H^+: (-1)K^+$ per transport cycle [6–8]. All these published studies have been performed in the absence of chloride to avoid contaminating the measurement of the transporter current by the uncoupled chloride current, which is transmitted via an anionic channel associated with glutamate transporters [9,10]. However, the possibility of GTS variation with changes in glutamate concentration has never been explored.

There are four variants of GLT-1. Alternative splicing at 3'-ends of GLT-1 message leads to two splice variants: GLT-1a and GLT-1b, also known as GLT-1v, with different C-termini that are expressed in rat liver [11] and brain [12–15]. GLT-1b interacts with the synaptic PDZ domain protein PICK1 [16]. The third carboxyl-terminal splice-variant is GLT-1c that is found within the retina and in the synaptic terminals of both rod- and cone-photoreceptors in both humans and rats [17]. The fourth splice variant is an exon 9-skipping form of GLT-1a that is expressed primarily in populations of white matter astrocytes [18]. Remarkably, GLT-1a protein has been also found expressed in excitatory axon terminals in the CA3 and CA1 fields of the rat hippocampus [14,19,20] and elsewhere [21] where extracellular glutamate concentration varies dramatically during glutamatergic neurotransmission.

Extracellular glutamate concentrations in the synaptic cleft of glutamatergic synapses vary by five orders of magnitude from the resting 25 nM [22] to above 1 mM during normal excitatory transmission [23–25] and even higher during burst activity [26]. Such enormous variations in synaptic cleft glutamate concentration may affect GTS of synaptically and perisynaptically expressed GLT-1a during excitatory transmission. Previously we found that in primary neuronal cultures and GLT-1a transfected COS-7 cells, GLT-1 coupled transporter current exhibits a statistically significant decrease while [3H]-L-glutamate uptake monotonically increases when extracellular glutamate concentrations rises from 100 to 300 μM [27]. This change in the current/flux ratio implies GTS variation or in other words "slippage" of the transport coupling in this particular glutamate concentration range. Similar "slippages" in transport stoichiometry have been observed in other transporters including the bacterial lactose transporter, LacY [28], the ClC-ec1 H^+-Cl^- exchange transporter [29], the dopamine transporter [30], the norepinephrine transporter [31], the serotonin transporter [32–34], and the Na^+/Ca^{2+} exchanger [35].

Notably, the transport rate of the human homolog of rodent GLAST, EAAT1, at 300 μM glutamate had been found smaller relative to its rate at both 200 μM and 1000 μM (see Fig 5B in [36]), which is comparable to what we found for the GLT-1 coupled current [27]. However, the decrease in EAAT1 was not statistically significant due to the large errors of the means.

Interestingly, in the following Fig 8D in [36], the authors presented the concentration dependence of the time constant for activation of L-glutamate currents, but without the 300 μM datum point. Therefore, our work clarifies the transport properties of GLT-1 specifically near 300 μM glutamate.

In the GTS studies of EAAT3, the coupled current was measured at 5, 10, 30, 100 and 300 μM, while the EAAT3 reversal potential was determined at the same concentrations, but not at the "critical" 300 μM. In addition, the data potentially allowed authors to determine GTS at three different concentration ranges: (5–10), (10–30), and (30–100) μM glutamate (see Figs 2F, 3A and 4A in [6]), by measuring ratios of the changes in the transporter reversal potential to the changes in the Nernst potential for glutamate in each of these ranges. The authors may have found that the slope in the lower concentration range (5–10 μM) was larger than in the middle (10–30 μM) range, as is noticeable in Figs 3A and 4A. However, the authors determined the EAAT3 stoichiometric ratio only across the entire glutamate concentration range, 5–100 μM. The reason is likely to be due to relatively large errors of the means of EAAT3 reversal potential measurements at individual glutamate concentrations, which would lead to large errors in the determination of the slopes and the stoichiometric ratios in these three concentration ranges. Interestingly, the measurement of the transporter reversal potential at the critical 300 μM glutamate was not communicated in this paper. It is possible that the reversal potential at 300 μM did not lie along the single fitting line with other the measurements in Fig 3A, and therefore would tend to indicate a change in the slope and in the stoichiometry, which would contradict the constant transport stoichiometry paradigm. This is another reason to measure GTS in at least two different glutamate concentration ranges around 300 μM.

GLT-1 stoichiometry has been previously determined, but also at a single glutamate concentration range, 100–300 μM [7]. Likewise, GLAST stoichiometry has been measured over a single range, 200–1000 μM [8]. Obviously to elucidate whether GTS of a transporter varies, one needs to know at least two different values of GTS measured in two different glutamate concentration ranges, which has never been done before.

Our previous report on the "slippage" of the transport coupling was conducted in the presence of Cl⁻ ions. Here we wanted to definitively ascertain the complete GTS across all relevant glutamate concentrations, and to do this we were compelled to omit Cl⁻. We evaluated GLT-1 transport stoichiometry at two different glutamate concentration ranges, in the absence of Cl⁻, which required measurements of GLT-1 reversal potential at a minimum of four different glutamate concentrations: two below and two above 200 μM. To clarify whether, at high glutamate concentration, GLT-1 operates in a channel-like mode, when GLT-1 thermodynamic parameter Q_{10} might diminish closer to 1, we measured the glutamate concentration dependence of the Q_{10} of the GLT-1 coupled transporter current. Our data show that in the absence of chloride, GLT-1 GTS remains constant over a wide 19–1,200 μM glutamate concentration range and over the same range shows a value of Q_{10} = 2.4. Surprisingly, the previously observed evidence for slippage of the GLT-1 coupled current was found to be dependent on the presence of chloride.

Materials and Methods

Assessment of GLT-1 transport stoichiometry

Here we assigned the reversal potential of GLT-1 as E_{rev}, GLT-1 coupled current as i, and membrane potential as ϕ. In the linear approximation we can write

$$i = g(\phi - E_{rev}) \tag{1}$$

where g is apparent stoichiometric (not-anionic) conductance of GLT-1 transporter.

At the reversal potential, $\phi = E_{rev}$, the current is zero and there is no change in total energy of the system per transport cycle. In this case, the change of the total energy alteration per cycle is equal to sum of changes in electrical and thermodynamic energies of transported ions and molecules, i.e. $\Sigma(n_j z_j)e\phi + \Sigma(n_j U_j / N_A) = 0$. Where, n_j – number of ions type "j" transported per cycle, z_j–j-ion valence, e–elementary positive charge (1.6×10^{-19} coulombs), U_j–transmembrane thermodynamic potential of j-ions that is equal to RT ln [(intracellular j-ion concentration) / (extracellular j-ion concentration)], and N_A–the Avogadro constant (6.02×10^{23} mole^{-1}). If all transported species are ions with non-zero charge, which is the case for GLT-1, the equilibrium at $\phi = E_{rev}$ can be rewritten in the following form:

$$\Sigma(n_j z_j)eE_{rev} - \Sigma(n_j z_j eE_j) = 0 \qquad (2)$$

where, $E_j = -U_j / (z_j F)$–is Nernst equilibrium potential of "j"-ion.

Note that $U_j = -z_j FE_j$.

From Eq 2 we find that

$$E_{rev} = \Sigma(n_j z_j E_j)/\Sigma(n_j z_j) \qquad (3)$$

Thus, E_{rev} for a glutamate transporter can be calculated as:

$$E_{rev} = (n_{Na}E_{Na} + n_H E_H + n_K E_K - n_{Glu}E_{Glu})/(n_{Na} + n_H + n_K - n_{Glu}) \qquad (4)$$

Here we have $z_{Na} = z_H = z_K = +1$, $z_{Glu} = -1$. For example, in case of generally accepted GTS we have $n_{Na} = 3$, $n_H = 1$, $n_{Glu} = 1$, $n_K = -1$, and $n_e = (n_{Na} + n_H + n_K - n_{Glu}) = +2$.

If glutamate is transported in neutral form, as a zwitterion, and free protons are not transported at all, then E_{rev} will depend on concentration of neutral glutamate ($[Glu^0]$) but not on pH directly. However, pH will affect $[Glu^0]$. In this case we have: $n_H = 0$, $z_{Glu} = 0$, and the E_{Glu0} is indeterminate. Therefore, in Eq 3 we need to replace E_{Glu0} with U_{Glu0}.

$$E_{rev} = \left\{n_{Na}E_{Na} + n_K E_K - n_{Glu0}\left((RT/F)ln\left(\left[Glu^0\right]_i / \left[Glu^0\right]_e\right)\right)\right\}/(n_{Na} + n_K) \qquad (5)$$

For further consideration, we will take the generally accepted view that only the ionic form of glutamate is transported by GLT-1. When extracellular concentration of transported ion changes, E_{rev} changes too, and its shift can be calculated. For example, if we change the sodium concentration in Eq 4 then:

$$\Delta E_{rev,Na} = n_{Na}\Delta E_{Na}/(n_{Na} + n_H + n_K - n_{Glu}) \qquad (6)$$

Therefore,

$$n_{Na}/(n_{Na} + n_H + n_K - n_{Glu}) \equiv n_{Na}/n_e = \Delta E_{rev,Na}/\Delta E_{Na} \equiv \Psi_{Na} \qquad (7)$$

We use Ψ_{Na} as an abbreviation for the experimentally determined ratio of the shift of GLT-1 reversal potential to the shift of sodium Nernst potential. Remarkably, it is equal to the ratio of the number of the transported ions per one transported positive elementary charge.

Similar relations can be determined for the all remaining 3 ions:

$$n_H/(n_{Na} + n_H + n_K - n_{Glu}) \equiv n_H/n_e = \Delta E_{rev,H}/\Delta E_H \equiv \Psi_H \tag{8}$$

$$n_K/(n_{Na} + n_H + n_K - n_{Glu}) \equiv n_K/n_e = \Delta E_{rev,K}/\Delta E_K \equiv \Psi_K \tag{9}$$

$$n_{Glu}/(n_{Na} + n_H + n_K - n_{Glu}) \equiv n_{Glu}/n_e = -\Delta E_{rev,Glu}/\Delta E_{Glu} \equiv \Psi_{Glu} \tag{10}$$

Thus, the number of transported sodium ions per one transported glutamate is equal to:

$$n_{Na}/n_{Glu} = (n_{Na}/n_e)/(n_{Glu}/n_e) = \Psi_{Na}/\Psi_{Glu} \tag{11}$$

Similarly, we can determine the ratios for other ions:

$$n_H/n_{Glu} = \Psi_H/\Psi_{Glu} \tag{12}$$

$$n_K/n_{Glu} = \Psi_K/\Psi_{Glu} \tag{13}$$

Interestingly, since $n_{Na} + n_H + n_K - n_{Glu} = n_e$, then the experimental values should be in agreement with the following theoretical equation:

$$n_{Na}/n_e + n_H/n_e + n_K/n_e - n_{Glu}/n_e = \Psi_{Na} + \Psi_H + \Psi_K - \Psi_{Glu} = 1 \tag{14}$$

Therefore, generally excepted stoichiometric ratios give us the anticipated result: 1.5 + 0.5–0.5–0.5 = 1. Our data gave us also the same result: 1.6 + 0.5–0.6–0.5 = 1.0. Thus, by measuring shifts of E_{rev} of the transport and knowing changes of ionic concentrations associated with them we can unambiguously determine the complete stoichiometry of the transporter.

The stoichiometric ratios calculated from E_{rev} shifts published for different glutamate transporters and those found for GLT-1 in this study are presented in Table 1.

Neuronal cultures

The Children's Hospital Institutional Animal Care and Use Committee (IACUC) approved this study. Neuronal cultures were prepared from embryonic day 16 Sprague Dawley rat fetuses as described previously [12,37]. Contamination by astrocytes was determined by immuno-chemical labeling with anti-glial fibrillary antibody and was found to be < 0.2% of total cells. Cultured neurons were used in electrophysiological experiments between 14 to 28 days *in vitro*.

Table 1. Stoichiometric transport ratios of glutamate transporters in the absence of chloride that have been reported previously and found here.

Transporter	[Glu]$_e$ (µM) range	Major anion	Temperature (°C)	n_{Na}/n_e	n_{Glu}/n_e	n_H/n_e	n_K/n_e	Source
EAAT3	5–100	Gluconate	Unspecified	1.70	0.54	0.42	-0.53	Zerangue et al., 1995
GLT-1	100–300	Gluconate	Unspecified	1.52	0.50	0.52	-0.39	Levy et al., 1998
GLAST	200–1000	Gluconate	Unspecified	1.37	0.43	0.40	-0.40	Owe et al., 2006
GLT-1	19–75	D-gluconate	37	1.56 ±0.23	0.50 ±0.02	0.48 ±0.06	-0.60 ±0.05	This study
GLT-1	300–1200	D-gluconate	37	1.48 ±0.13	0.52 ±0.04	0.48 ±0.03	-0.58 ±0.06	This study
GLT-1	19–75	D-gluconate	26	1.44 ±0.20	0.48 ±0.02	0.37 ±0.07	-0.60 ±0.12	This study
GLT-1	300–1200	D-gluconate	26	1.33 ±0.20	0.46 ±0.05	0.43 ±0.06	-0.65 ±0.10	This study

[Glu]$_{e,1}$ and [Glu]$_{e,2}$ are two glutamate concentrations which were used to determine number of glutamate molecules transported per one elementary charge (e$^+$) in an appropriate study. Data are shown as mean ± s.e.m.

doi:10.1371/journal.pone.0136111.t001

Transient transfection of COS-7 cells by EGFP and GLT-1a cDNAs

For GLT-1a stoichiometric measurements we used COS-7 cells, which is a African green monkey kidney fibroblast-like cell line [38] suitable for transfection by vectors requiring expression of SV40 T antigen (ATCC, catalog No. CRL-1651). 0.3 million wild type COS-7 cells were plated per 35 mm dishes in VP-SFM (cat. # 11681–020, Invitrogen, Carlsbad, CA) with 4 mM L-glutamine. In 24 hours cell medium in each dish was replaced with 2.4 ml Opti-MEM (cat. # 31985–062, Invitrogen) containing 4 μg GLT-1a and 1 μg EGFP cDNAs [12] and 12 μl Lipofectamine 2000 (cat.# 11668–019, Invitrogen) for 5 hours. Then the transfection medium was replaced with VP-SFM containing 0.1 mM L-glutamine. After 24–72 hour the transfected COS-7 cells with maximum EGFP fluorescence were selected for the patch-clamp experiments using fluorescent DIAPHOT 200 inverted microscope (Nikon, Japan). In separate experiments, COS-7 cells were transfected with EGFP only for control patch-clamp experiments.

Electrophysiology

There are two different currents generated by GLT-1 that are activated by glutamate. The current of interest is stoichiometrically coupled with glutamate transport, but another current is uncoupled with the glutamate transport and generated by chloride ions passing through anionic channel inside the transporter [3]. In the experimental solutions where chloride was the major anion, we excluded the uncoupled anionic current by nullifying the driving force for chloride. This was accomplished by equalizing the Nernst equilibrium potential for chloride (E_{Cl}) to the holding membrane potential (HP) of −70 mV. In these conditions the current generated by GLT-1 was only the coupled glutamate transporter current (i_{Glu}).

Electrophysiological experiments were performed in the whole cell configuration with WPC-100 amplifier (E.S.F., Germany), pClamp 10 software (Molecular Probes, USA), and MP-225 micromanipulator (Sutter Instrument, USA). Only cell with more than 5 GOm seal resistance at cell-attached configuration were used in the experiments to minimize leak current and improve signal to noise ratio for the small GLT-1 current. Temperature of the chamber (Cat. # TC-344B, Warner Instruments) was adjusted to 37°C or to 26°C as described below. Extracellular solution exchange was performed with computer controlled fast solution application system (Cat. # PC-1, Bioscience Tools, USA) with 8-channel heated micromanifold MPRE8 (Cell MicroControls, USA) that allowed to change solution around a studied cell within 300 ms and adjust solution temperature with 0.1°C accuracy. The temperature of the solution coming from the manifold was also adjusted to 37°C or to 26°C, accordingly to appropriate experimental protocols. The control solution was always applied before and after each experimental solution to minimize effect of the base line drift and improve accuracy of GLT-1 reversal potential (E_{rev}) measurements. Several current records obtained during subsequent applications of the same set of solutions were later averaged to improve signal to noise ratio.

Membrane conductance was determined as an average of two conductances at positive and negative slopes of the voltage ramp in -70 to -30 mV regions. The changes in the membrane capacitance were determined from the differences of the currents at positive and negative slopes of the voltage ramp according to equation: $\Delta C = \Delta I/\Delta(dV_m/dt)$.

Solutions

Artificial cerebrospinal fluid (ACSF) contained (in mM): 160 NaCl, 2.5 KCl, 2.5 CaCl$_2$, 1.3 MgCl$_2$, 10 D-glucose, 10 HEPES (pH 7.4, adjusted with N-methyl-D-glucamine). The intracellular solution contained (in mM): 1 NaCl, 110 KOH, 20 tetraethylammonium (TEA), 1 CaCl$_2$, 5 MgCl$_2$, 5 EGTA, 10 HEPES (pH 7.2 was adjusted with gluconic acid). Osmolality in all solutions was measured with (Wescor vapor pressure osmometer Model 5520, Logan, UT, USA)

and adjusted to 330 mmol/kg with mannitol. With these solutions E_{Cl} = -70 mV that allows us to nullify GLT-1 uncoupled chloride current at HP = −70 mV. In addition, intracellular potassium was adjusted to obtain E_K = -70 mV, by replacement with N-methyl-D-glucamine to nullify all currents through the potassium channels to increase signal to noise ratio for GLT-1 couple current measurements. In experiments with cultured cerebral neurons, all ionotropic glutamate receptors were blocked with 10 µM (*RS*)-3-(2-carboxypiperazin-4-yl)-propyl-1-phosphonic acid (CPP), 100 µM 5,7-dichlorokynurenic acid, 10 µM 2,3-dioxo-6-nitro-1,2,3,4-tetrahydrobenzoquinoxaline-7-sulfonamide (NBQX), and 50 µM 4-(8-methyl-9*H*-1,3-dioxolo[4,5-h][2,3]benzodiazepin-5-yl)-benzenamine (GYKI 52466) [39]. Endogenous neuronal electrical activity was blocked with 0.3 µM TTX. To reduce GABA associated noise we added 25 µM bicuculline.

To measure shifts of GLT-1 E_{rev} we used GLT-1a transfected COS-7 cells that have no glutamate activated channels and high expression level of GLT-1a. In intra- and extracellular solutions all chloride was substituted with D-gluconate, an impermeable anion. Chloride ions are required for current transduction at the solution to silver-chloride pellet interface. Durations of all our experimental protocols were less than 100 seconds, and the average GLT-1 current was always below 1000 pA. Therefore, total required transmitted charge was less than 10^{-7} C, corresponding to 1.04 pmol of Cl^- as the charge carrier, which in 10 µl of the pipette solution translates into approximately 100 nM for the pipette Cl^- concentration. Such a miniscule amount of chloride in the pipette solution might come either from the traces of chloride in the salts used to make up the solution or from chloride dissociation from the silver-chloride pellet during the several minutes before the start of an experiment. The solution for the electrical connection with the reference electrode was ACSF with high chloride concentration. The chloride-free extracellular solution contained (in mM): 102 Na D-gluconate, 44 K D-gluconate, 10 D-glucose, 15 HEPES, pH 7.4 adjusted with N-methyl-D-gluconate. Concentrations of free calcium and magnesium were adjusted to 1 mM and 2 mM, respectively, with $Ca(D-gluconate)_2$ and $Mg(D-gluconate)_2$, and confirmed by measurements with ion-selective electrodes. The intracellular solution in these experiments contained (in mM): 20 Na D-gluconate, 10 Na L-glutamate, 100 K D-gluconate, 20 TEA, 5 EGTA, 20 HEPES, pH 7.0 adjusted with D-gluconic acid. Concentrations of free calcium and magnesium were adjusted to 100 nM and 4 mM with $Ca(D-gluconate)_2$ and $Mg(D-gluconate)_2$, respectively, and measured with ion-selective electrodes. Osmolality in all solutions was adjusted to 330 mmol/kg with mannitol. To determine the ion specific shift of the GLT-1 E_{rev}, the following ionic concentrations were changed in separate experiments: 1) $[Na^+]_e$ from 102 to 51 mM, 2) $[K^+]_e$ from 42.5 to 10.6 mM, and 3) $[H^+]_e$ from 40 to 10 nM (that corresponds to a pH shift from 7.4 to 8.0) in the presence of 37.5 or 600 µM glutamate. Since the inhibition of GLT-1 by DHK is competitive, we have used higher DHK concentrations at higher glutamate concentrations to determine E_{rev} of DHK sensitive current more accurately that is described in details in appropriated sections below.

Statistics and fitting of the data

Experimental data in the figures and in the text are presented as mean ± s.e.m. Two-tailed t-test was used to determine statistical significance of the effects.

For comparison of the ratios of GLT-1 current in the presence and the absence of chloride to appropriate flux data in the presence of chloride obtained previously [27], we have normalized the data at 100 µM glutamate to corresponding values at 300 µM glutamate. In curve fittings, we used Origin (version 6; Microcal Software Inc.).
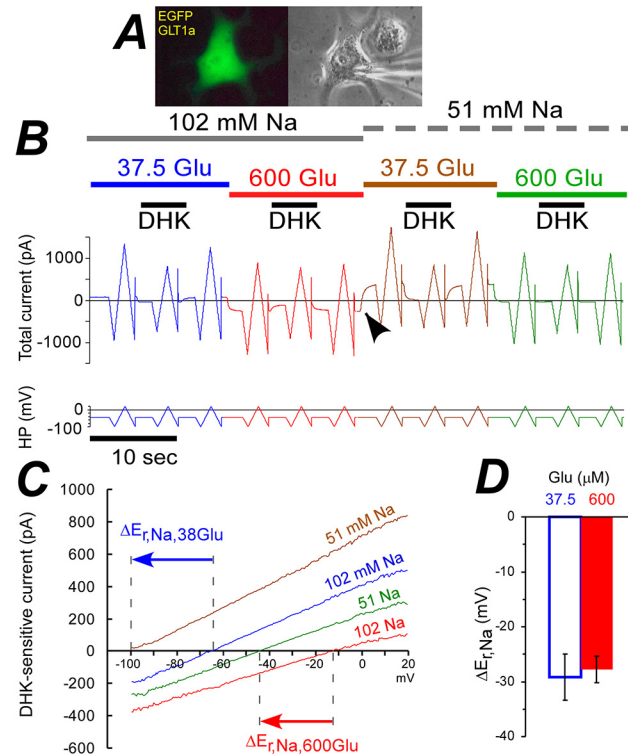
Fig 1. In the absence of chloride, two-fold decrease in $[Na^+]_e$ shifted GLT-1a E_{rev} by –28 mV at both low and high glutamate concentrations. (A) Fluorescent (left) and phase-contrast (right) images of COS-7 cell expressing both EGFP and GLT-1a. **(B)** Representative data show total membrane current, the time courses of $[Na^+]_e$, $[Glu^-]_e$, and $[DHK]_e$ at the top, and HP voltage ramps (–100 to +20 mV) at the bottom. Arrow head points to simultaneous decrease in $[Glu^-]_e$ and $[Na^+]_e$, which affects the current. **(C)** I-V curves of DHK sensitive currents obtained form **(B)** as a result of subtractions of averages of 2 I-V curves in presence of DHK from averages of 4 I-V curves in the absence of DHK at corresponding $[Glu^-]_e$ and $[Na^+]_e$. Arrows show amplitudes and directions of E_{rev} shifts associated with decrease in $[Na^+]_e$. **(D)** Average E_{rev} shifts at $[Glu^-]_e$ geometric means of 37.5 and 600 µM are approximately equal when $[Na^+]_e$ was decreased from 102 to 51 mM. Data here and in all following bar graphs are shown as mean and SEM.

doi:10.1371/journal.pone.0136111.g001

Results

How many Na^+ ions does GLT-1 transport per one positive elementary charge (e^+)?

Previously we observed decrease in n_e/n_{Glu} at high glutamate concentrations measured in the presence of chloride [27]. Such a change might be due to an increase in n_{Glu}, but also might be due to changes in n_{Na}, n_H, or n_K, which all affect n_e. To determine exact GLT-1 GTS at both low and high glutamate concentrations we used COS-7 cells transiently transfected with both GLT-1a and enhanced green fluorescent protein (EGFP) (Fig 1A). All stoichiometric experiments were performed in chloride-free solutions to avoid possible contamination of the measured coupled transporter current by the uncoupled anionic current.

The calculations of GLT-1 stoichiometric ratios from the shifts of its reversal potential are described in the Methods section. E_{rev} was determined as the zero-current potential of the current blocked by 600 or 700 µM DHK at 37.5 or 600 µM glutamate, respectively (Fig 1B and 1C). When $[Na^+]_e$ was decreased 2 times (replacement by non-permeable N-methyl-D-gluconate), E_{rev} shifted by approximately 28 mV in the negative direction at both 37.5 and 600 µM
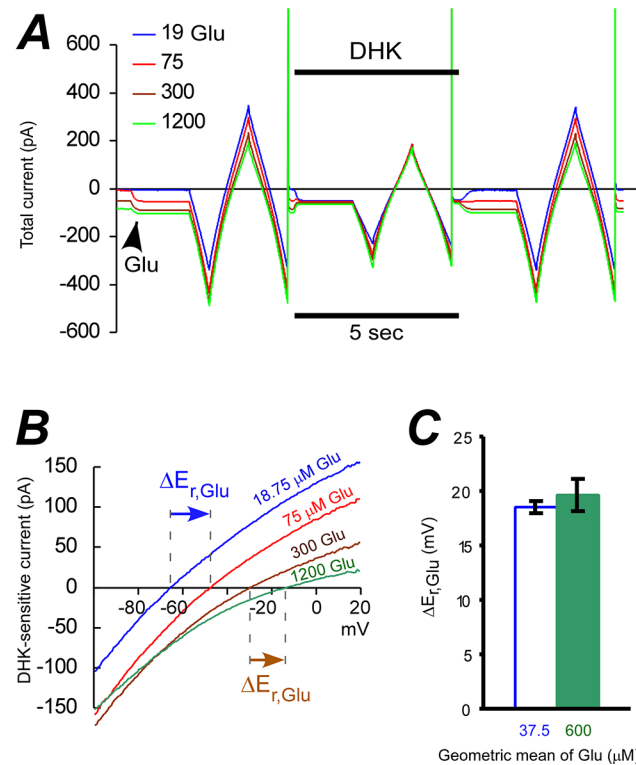
Fig 2. Four-fold increase in [Glu⁻]ₑ shifted GLT-1a Eᵣₑᵥ by +19 mV at both low and high glutamate concentrations. (A) Representative experiment shows responses of the total current to the voltage ramp (−100 to +20 mV) at different [Glu⁻]ₑ in the absence and the presence of DHK. Arrow head shows onset of next glutamate concentration application. **(B)** I-V curves of DHK sensitive currents obtained form **(A)**. Arrows show Eᵣₑᵥ shifts. **(C)** Average GLT-1 Eᵣₑᵥ shifts at [Glu⁻]ₑ geometric means of 37.5 µM and 600 µM are approximately equal when [Glu⁻]ₑ was increased from 18.75 to 75, or from 300 to 1200 µM, respectively.
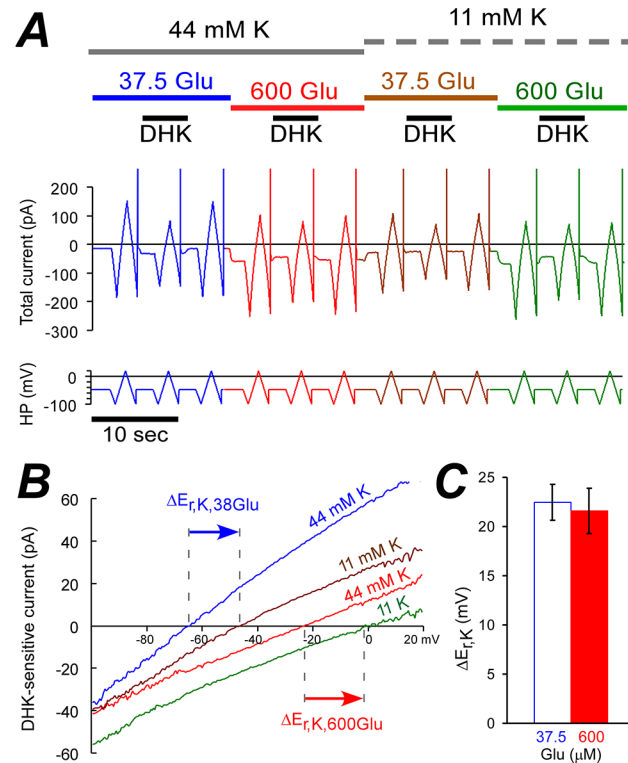
doi:10.1371/journal.pone.0136111.g002

glutamate concentrations ([Fig 1D](#)). Thus, n_{Na}/n_e ratio is the same at both low and high glutamate concentrations; $n_{Na}/n_e = \Delta E_{rev}/\Delta E_{Na} \approx$ (-28 mV) / (RT/F ln(51/102)) ≈ 1.5.

GLT-1 transports one Glu⁻ per two e⁺ at low and high [Glu]ₑ

The n_{Glu}/n_e ratios were determined by measuring the ΔE_{rev} of the DHK sensitive current when [Glu⁻]ₑ was increased from 18.75 to 75, to 300, and to 1200 µM. Due to the competitive nature of DHK inhibition, we used increasing concentrations of [DHK]ₑ ([Fig 2A](#)). The first four fold increase in [Glu⁻]ₑ from 18.75 to 75 µM, corresponding to the geometric mean of 37.5 µM, led to approximately 19 mV shift of the Eᵣₑᵥ of DHK-sensitive current in positive direction ([Fig 2B](#)). Similarly, the last four fold increase in [Glu⁻]ₑ, with its geometric mean equal to 600 µM, led to the same ΔE_{rev} ([Fig 2C](#)). Therefore, $n_{Glu}/n_e = -\Delta E_{rev}/\Delta E_{Glu} \approx$ (+19 mV) / (RT/F ln(4)) $\approx$ 0.5 in both examined glutamate concentration ranges. Surprisingly, these results challenge our own current/flux studies where the ratio at high glutamate concentration was approximately two times lower than at low concentration. However, our previous current/flux studies were performed in the presence of chloride [27], which we will address below.

GLT-1 cycle time is 52 ms in the absence of chloride

The experiments shown in [Fig 2](#) allowed us to determine the membrane capacitance at each pair of positive and negative holding potential (HP) ramps as described in the Methods section.

Fig 3. Four-fold decrease in $[K^+]_e$ shifted GLT-1a E_{rev} by +22 mV at both low and high glutamate concentrations. (A) Representative experiment shows the current with the identifying clues as in Fig 1B. (B) I-V curves of DHK sensitive currents obtained form (A). Arrows show GLT-1a E_{rev} shifts. (C) Average GLT-1 E_{rev} shifts at 37.5 µM and 600 µM are approximately equal when $[K^+]_e$ was decreased from 44 to 11 mM.

doi:10.1371/journal.pone.0136111.g003

We found that at 37°C, −50 mV and 1200 µM glutamate, the ratio of the DHK-sensitive GLT-1 current to DHK-sensitive capacitance is equal to 4.6±0.4 (A/F = V/s). Therefore, at −50 mV the ratio of the current to GLT-1-specific capacitive charge is equal to (4.6 V s^{-1}) / (50 mV) = 92±8 s^{-1}, which is close to the value of 70 s^{-1} found at − 80 mV and 1000 µM glutamate for human EAAT2 [40]. This number (92±8 s^{-1}) would correspond to the charge transfer rate if the GLT-1 capacitive charge would be equal to an elementary charge and sensed the whole membrane potential. However, assuming that the product of the valence of the capacitive charge and the apparent fraction of the field sensed by the charge (zδ) in GLT-1 is the same as in EAAT2 and equal to 0.41 [40], the number of elementary charges transported at −50 mV per sec by GLT-1 is 38±3 s^{-1}, which is relatively close to the value of 29 s^{-1} shown for EAAT2 at −80 mV [40]. Therefore, when GLT-1 transports 2 elementary charges per cycle ($2 = +3_{Na} - 1_{Glu} + 1_H - 1_K$), its cycle time is equal to 52±4 ms, which corresponds to the turn-over rate of 19±2 s^{-1}.

GLT-1 counter-transports one K^+ ion per two e^+ at low and high $[Glu]_e$

These experiments were similar to those described in Fig 1, with different $[K^+]_e$ applied as shown in Fig 3A. We used 600 or 700 µM DHK at 37.5 or 600 µM glutamate, respectively (Fig 3A and 3B). When extracellular potassium concentration was decreased four times from 44 to 11 mM, E_{rev} of the DHK sensitive current shifted by 22.5±1.8 mV and by 21.6±2.3 mV in positive direction for 37.5 and 600 µM glutamate, respectively (Fig 3C). Therefore, n_K/n_e ratio is

essentially the same for both low and high glutamate concentrations. That is $n_K/n_e = \Delta E_{rev}/\Delta E_K \approx$ (+22 mV) / (RT/F ln(11/44)) $\approx$ -0.57.

GLT-1 transports one proton per two e$^+$ at low and high [Glu]$_e$

We have determined the effect of the proton concentration on GLT-1 E_{rev} as shown in Fig 4A. We used 600 or 700 μM DHK at 37.5 or 600 μM glutamate, respectively (Fig 4A and 4B). When extracellular proton concentration was decreased four times from 40 to 10 nM (i.e. pH was increased from 7.4 to 8.0), E_{rev} of the DHK sensitive current shifted by 18±2 mV and by 18±1 mV in negative direction for 37.5 and 600 μM glutamate, respectively (Fig 4C). Therefore, n_H/n_e ratio is the same for both low and high glutamate concentrations; i.e., $n_H/n_e = \Delta E_{rev}/\Delta E_H$ = (-18 mV) / (RT/F ln(10/40)) = 0.48.
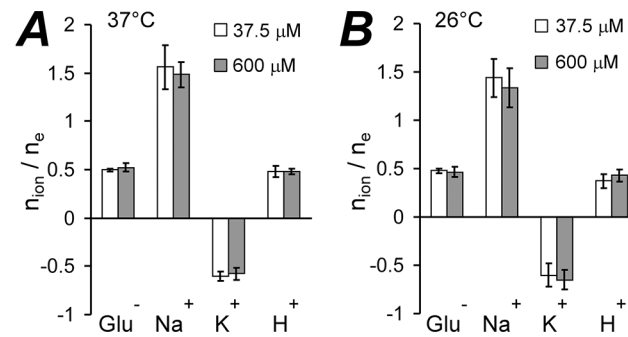
In the absence of chloride GLT-1 GTS does not depend on temperature

So far the data imply that in the absence of chloride, the transport stoichiometry at 37°C remains the same at both 37.5 and 600 μM glutamate (Fig 5A). This is in agreement with the generally accepted point of view, but does not support our previous data [27] where we discovered slippage of GLT-1 current-flux coupling at 37°C with k_D = 0.17 mM glutamate and n_{Hill} = 3.2. Some investigators have not specified the temperature used in their studies of GTS (see Table 1), and therefore we conducted a similar set of stoichiometric experiments at 26°C. However, GLT-1 GTS still remained constant even at the lower temperature (Fig 5B).
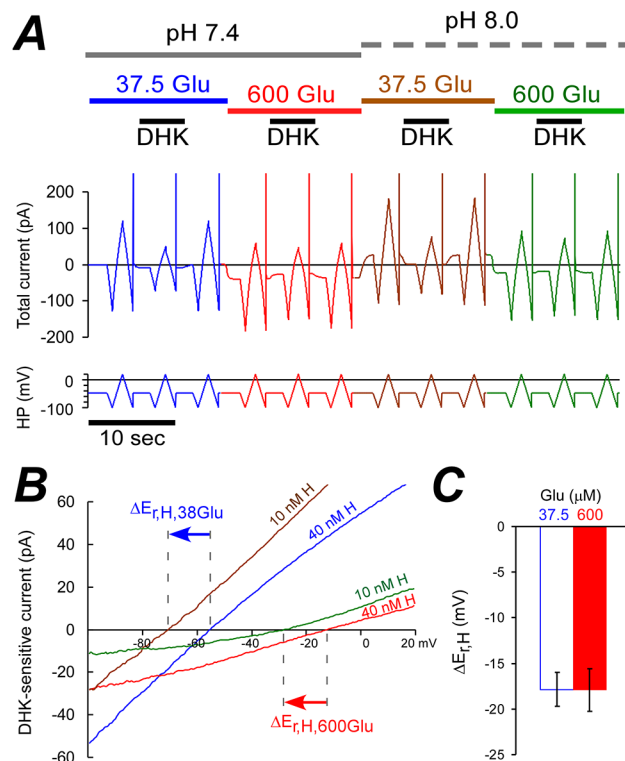
Fig 4. Four-fold decrease in [H$^+$]$_e$ shifted GLT-1a E_{rev} by −18 mV at both low and high glutamate concentrations. (A) Representative experiment shows the current as in Fig 1B. (B) I-V curves of DHK sensitive currents are obtained form (A). Arrows show GLT-1a E_{rev} shifts. (C) Average GLT-1 E_{rev} shifts at 37.5 μM and 600 μM are approximately equal when [H$^+$]$_e$ was decreased from 40 to 10 nM.

doi:10.1371/journal.pone.0136111.g004

Fig 5. In the absence of chloride, GLT-1 glutamate transport stoichiometry remains constant at low and high glutamate concentrations, as well as at different temperatures. (A) GLT-1 transport stoichiometry at 37°C at low (open bars) and high (grey bars) glutamate concentrations. For pair of transported elementary charges GT1 co-transports approximately one glutamate, three sodium ions, and one proton, and counter-transports one potassium ion. **(B)** GLT-1 transport stoichiometry at 26°C at low (open bars) and high (grey bars) glutamate concentrations. The stoichiometry is the same as at 37°C and approximately has the following transport ratios: $n_{Glu}/n_{e+} = \frac{1}{2}$, $n_{Na+}/n_{e+} = 3/2$, $n_{K+}/n_{e+} = -\frac{1}{2}$, and $n_{H+}/n_{e+} = \frac{1}{2}$.

doi:10.1371/journal.pone.0136111.g005

In the absence of chloride, Q_{10} for GLT-1 transport does not depend on $[Glu]_e$

We measured Q_{10} for GLT-1 coupled current in 10 μM– 10 mM glutamate concentration range (Fig 6). The Q_{10} value remained constant ($Q_{10} = 2.4\pm0.1$) over the whole range, and does not comes close to the value for passive diffusion where $Q_{10} \approx 1.3$. This is in agreement with constant transport stoichiometry, and does not provide evidence for slippage of the current-flux coupling, because slippage is usually associated with channel-like behavior of a transporter and a lower Q_{10} value.

Removal of chloride eliminates slippage of transport coupling in cultured neurons

The major difference in the present stoichiometric experiments compared to our previous experiments was the absence of chloride, leading to the hypothesis that the substitution of gluconate for chloride in the present experiments eliminated the slippage phenomenon. To test this hypothesis, we determined the coupled GLT-1 current-glutamate concentration dependence as we have previously [27], but with chloride replaced with gluconate. Surprisingly, we found that the decrease in the coupled transporter current in the 100–300 μM glutamate concentration range in GLT-1a transfected COS-7 cells was NOT observed in the absence of chloride (Fig 6A–6D).

Our previous experiments were performed on primary neurons in culture [27]. The transporter current in cultured neurons significantly decreased in the 100–300 μM glutamate concentration range in the presence of chloride as has been described previously [27]. However, when we repeated similar experiments in the absence of chloride, we found that there was NO decrease in the transporter current in the same glutamate concentration range (Fig 7A). It should be noted that a non-saturating and GLT-1 non-specific current in the presence of chloride appears only at $[Glu]_e > 300$ μM, as it was shown in Figs 2D and 4C in [27]. Therefore, the increase in GLT-1 coupled current in neurons in the absence of chloride when $[Glu]_e$ increases from 100 to 300 μM, and the decrease of GLT-1 current in the presence of chloride at the same concentrations should be considered as GLT-1 specific effect of chloride ions on the transporter (Fig 7A).
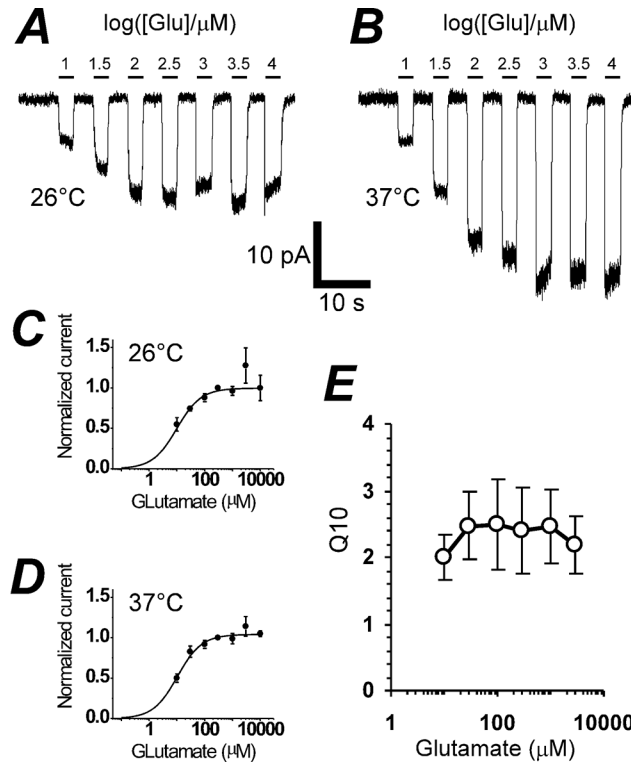
Fig 6. In the absence of chloride, Q_{10} of GLT-1a does not depend on glutamate concentration. (A) Representative experiment shows responses of GLT-1a stoichiometric current to wide range of glutamate concentrations (from 10 to 10^4 μM) at 26°C. **(B)** Glutamate responses of the same cell as in **(A)** at 37°C. The scaling bars are the same for **(A)** and **(B)**. **(C)** and **(D)** show cumulative data for 26°C and 37°C with glutamate $k_{D,26°C} = 9.9 \pm 1.6$ μM and $k_{D,37°C} = 10.3 \pm 1.5$ μM, respectively. (*E*) Glutamate dose dependence of Q_{10} of GLT-1a. The average value of Q_{10} for glutamate concentrations in the range from 30 μM to 10 mM is 2.4 ± 0.1.

doi:10.1371/journal.pone.0136111.g006

If we compare normalized ratios of the neuronal GLT-1 coupled current (in the presence and in the absence of chloride) to previously found values of [^{3}H]-L-glutamate fluxes carried
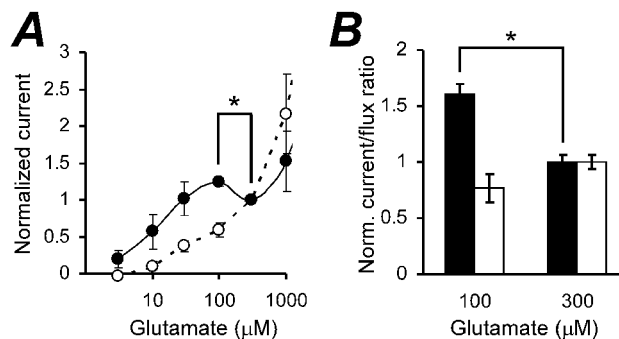
Fig 7. Replacement of intra- and extracellular chloride for D-gluconate eliminated statistically significant decreases in GLT-1 stoichiometric current and the current/flux ratio in 100–300 μM glutamate concentration range. (A) Normalized GLT-1 stoichiometric current glutamate concentration dependences in the presence chloride, E_{Cl} = HP = -70 mV, (solid circles), and in the absence of chloride (open circles). **(B)** Normalized current/flux ratios in the presence (black bars) and in the absence of chloride (white bars). Flux data are taken from [27]. *- corresponds to p < 0.05.

doi:10.1371/journal.pone.0136111.g007

by neuronal GLT-1 at 100 and 300 μM [27], we find that the slippage (i.e. significant change in the current/flux ratio at 300 μM glutamate) occurs only in the presence of chloride (solid bars in Fig 7B, p < 0.05), but not in the absence of chloride (open bars).

Discussion

GLT-1 GTS is constant with substitution of gluconate for chloride

Analysis of GLT-1 glutamate transport thermodynamic equilibrium allowed us to derive Eqs (7–10, see the methods) showing that the number of a particular type of ion (atom or molecule) transported per elementary charge is equal to the ratio of the transporter reversal potential shift to the particular ion's Nernst equilibrium potential shift. Our data indicate that in the absence of chloride, GLT-1 co-transports 1.5 Na^+, 0.5 Glu^-, 0.5 H^+ and counter-transports 0.6 K^+ per one transported elementary charge in both low (19–75 μM) and high (300–1200 μM) extracellular glutamate concentration ranges, and at both 26°C and 37°C temperatures (Figs 1–5). However, this is obviously inconsistent with the previously found slippage of transport coupling in GLT-1 at high glutamate concentrations in the presence of chloride [27], which we will discuss below.

The Q_{10} value of 2.4 remains constant in 30–10,000 μM glutamate concentration range (Fig 6), which is in agreement with the idea that GTS is constant and GLT-1 is not slipping into a channels-like mode when Q_{10} would diminish closer to 1. Found here Q_{10} value is close to the 2.9 value of Q_{10} for EAAT1 radiolabeled uptake [36]. This magnitude of Q_{10} is also in agreement with the temperature dependence of decay rate of synaptically activated transporter-mediated current in hippocampal astrocytes [26].

The apparent slippage of GLT-1 transport coupling is not an artifact

The inconsistency between the constant GLT-1 stoichiometry found here and the variable stoichiometry in the presence of chloride [27] (Fig 7) might be an artifact in the current-flux experiments. However, we already evaluated plausible artifacts in previously reported experiments [27]. Briefly, the transport "slippage" is not due to accumulation of intracellular submembrane glutamate that could attenuate the expected increase in transporter driving force due to glutamate diffusion limitation in the submembrane space [40], similar to the one found for ATP [41]. "Slippage" was also observed at 10 mM intracellular glutamate, when the relative change in intracellular submembrane glutamate concentration would be negligible. The slippage is also not due to a self-blocking effect of glutamate on its own influx as had been shown for $GABA_A$ receptors [42] because this would also decrease glutamate uptake, which did not occur. Likewise, it is not due to poor voltage camp that could lead to non-zero driving force for uncoupled chloride current [9] even when HP = E_{Cl}, because uncoupled current was found to be very small in EAAT2 [40,43], and in addition the "slippage" phenomenon was also observed in GLT-1a transfected COS-7 cells, which are geometrically compact and therefore have reliable spatial voltage clamp [27]. The COS-7 experiments also exclude any possibility of GluRs contribution because GluRs are not expressed in these cells.

Dependence of GLT-1 GTS on glutamate concentration depends on chloride

Previously [6–8], and here, GTS parameters have been determined in the absence of chloride to avoid the confound of a contribution from the uncoupled anionic transporter current to the measurements of the coupled current reversal potential. Yet, all previously published studies determined GTS only in a specified glutamate concentration range, and the possibility of GTS

variation was not considered. Since we have found evidence for the slippage in GLT-1 transport coupling at high glutamate concentrations [27], it was obligatory to clarify if the complete transport stoichiometry is different in two [Glu]$_e$ concentration ranges, specifically, below and above the apparent slippage phenomenon occurs. Unexpectedly, we found that GLT-1 GTS is the same in both low (19–75) and high (300–1200 μM) glutamate concentration ranges, as well as at both 37°C and 26°C temperatures (Fig 5). Specifically, when chloride is substituted by impermeable D-gluconate, GLT-1 GTS is $3Na^+$: $1Glu^-$: $1H^+$: $(-1)K^+$, which is in agreement with the original reports [6–8].

To clarify the nature of the inconsistency between the slippage in GLT-1 transport coupling [27] and constant GTS found here, we assessed the coupled transporter current as a function of glutamate concentration in the identical experiments as before [27], but in the absence of chloride. In this case, we observed no reduction of the coupled transporter current in 100–300 μM glutamate concentration range in both GLT-1a transfected COS-7 cells (Fig 6) and neurons (Fig 7). These data imply that both GLT-1 transport coupling and GTS are constant in the absence of chloride ions, but vary in the presence of chloride and high glutamate concentrations.

How to interpret effect of chloride on GLT-1 GTS?

There are at least two obvious possibilities that could potentially explain why GLT-1 transport coupling slippage occurs at high glutamate concentrations in the presence of chloride [27] and does not occur when chloride is absent (Figs 6 and 7). The first option is that chloride, but not D-gluconate, is required for a second glutamate transport with apparent k_D = 0.17 mM glutamate and glutamate binding cooperativity corresponding to n_{Hill} = 3.2 [27]. Noticeably, the latter matches n_{Hill} = 3 for the anionic uncoupled current of EAAT4, which occurs only at high transport cycling rate with 140 mM extracellular sodium, but not with 40 mM (see Fig 4B in [44]). Potentially, this rate-dependent cooperativity might occurs due to changes of local submembrane ion concentrations [41] and subsequent electrostatic or electromagnetic interference between coupled and uncoupled currents at the same transporter trimeric protein. For example, increase in the inward coupled current could produce a positive shift in the intracellular voltage, which could reduce the electrical component of the transporter driving force when chloride and anionic uncoupled current are absent. However, in the presence of chloride, simultaneous, but opposite uncoupled current in the same or neighboring subunit(s) of a transporter would reverse the local voltage alteration and restore (increase) the transporter driving force and plausibly allow the second glutamate molecule to be transported.

The second option could be that the impermeable D-gluconate (which was used to replace chloride anions) blocks a second glutamate binding site. D-gluconate is an organic anion as is glutamate. Since it is present at a thousand times higher concentration than glutamate, it plausibly might compete with glutamate for a second glutamate binding site even if it might have low affinity for the site. The major glutamate binding site is considered to be associated with a conserved NMDGT motif located on transmembrane domain (TM) 7 and arginine-477 on TM8 [45]. Overall, TM7 and TM8 and the two reentrant loops HP1 and HP2 participate in the formation of the binding pocket.

It has been shown that ultra-fast glutamate application causes fast inward transient current within 130 μs [46,47]. This implies that not only negatively charged glutamate moves into the transporter (outward current), but at least two positive ions (two Na^+ ions or Na^+ and H^+) also move into the transporter transmembrane electric field. Therefore, it might be possible that a second glutamate could bind to the same binding site as the first glutamate during the same transport cycle, but after 130 μs when the first glutamate moves into GLT-1 electric field and

vacates the site for the second glutamate. In this case, we could assume that the affinity of the original site for the second glutamate has $k_D = 0.17$ mM, and probability of the second transport mode [$3Na^+$: $2Glu^-$: $1H^+$: $(-1)K^+$] would be 50% at high glutamate concentration [27]. Therefore, the average GTS at high glutamate would be $3Na^+$: $1.5Glu^-$: $1H^+$: $(-1)K^+$, with $(n_{Glu} / n_e) = 1.5 / 1.5 = 1$, which is in agreement with the transport coupling slippage data.

An alternative option for the binding site for the second glutamate might be a completely different site, such as the DHK binding site, which is associated with S443 on external HP2 [48]. However, this would be a GLT-1 specific option, which is not available (with high affinity) for other glutamate transporters.

GLT-1 cycle time is 52 ms

Previously we deliberated that the second glutamate might bind to GLT-1 only after 130 µs, when the first glutamate moves into GLT-1 electric field. However, is GLT-1 transporter cycling time sufficiently long to allow the second glutamate binding within a single transport cycle? Here we showed that GLT-1 turnover rate at 37°C and −50 mV is 19 ± 2 s^{-1}, which is unsurprisingly faster than 15 s^{-1} turnover rate at 22°C and −80 mV for human EAAT2 expressed in *Xenopus* oocytes [40]. The difference is probably due to the effect of temperature on the turnover rate (Fig 6). In addition, glutamate transporters can effectively clear synaptic glutamate within 1 ms (perhaps via glutamate binding to the transporters), and the rise time (20%–80%) of the peak of the transporter current upon ultra-fast 1 mM glutamate application was found to be in the 0.1 ms range [46,47,49]. Therefore, 52 ms GLT-1 cycle time appears to be long enough for plausible binding of the second glutamate to the transporter.

However, an extremely short (a few milliseconds) time of synaptic glutamate concentration elevation might be too short for the binding of a second glutamate to GLT-1. Yet, sometimes the synaptic glutamate is elevated for tens of milliseconds, as in the case of long bursts of spikes [26], and then synaptic GLT-1 is exposed to high glutamate concentrations that can affect the decay kinetics of excitatory transmission and possibly synaptic plasticity [50] by binding and perhaps transporting two glutamate molecules per cycle and consequently accelerating synaptic glutamate clearance. Thus, one might expect that the second GTS mode makes a supplementary contribution to synaptic glutamate clearance during long excitatory bursts.

Physiological and pathophysiological implications of GLT-1 GTS changes

Accurate knowledge of GLT-1 transport stoichiometry is important for a detailed understanding of the role of GLT-1 in normal synaptic transmission, as well as in the pathophysiology of stroke. During normal physiological conditions, when high glutamate concentrations are attained, the existence of the second binding site would be expected to promote glutamate clearance. However, in the excitatory synapse compromised by energy failure, glutamate transport effectively reverses its normal direction of operation and releases glutamate. This reversal occurs when the membrane potential depolarizes above the GLT-1 reversal potential, which itself depends on GTS. Specifically, GLT-1 that transports two glutamate molecules per cycle will reverse earlier than GLT-1 transporting only one glutamate (Fig 8). The influence of GTS on the GLT-1 reversal potential may be especially relevant for excitotoxicity mediated via the relatively low affinity AMPA/kainate receptors, as in global ischemia [51], and in white matter injury in the developing brain [52]. However, the genuine GTS of GLT-1 across the whole synaptic glutamate concentration range and in the presence of physiological concentrations of chloride still requires further studies.
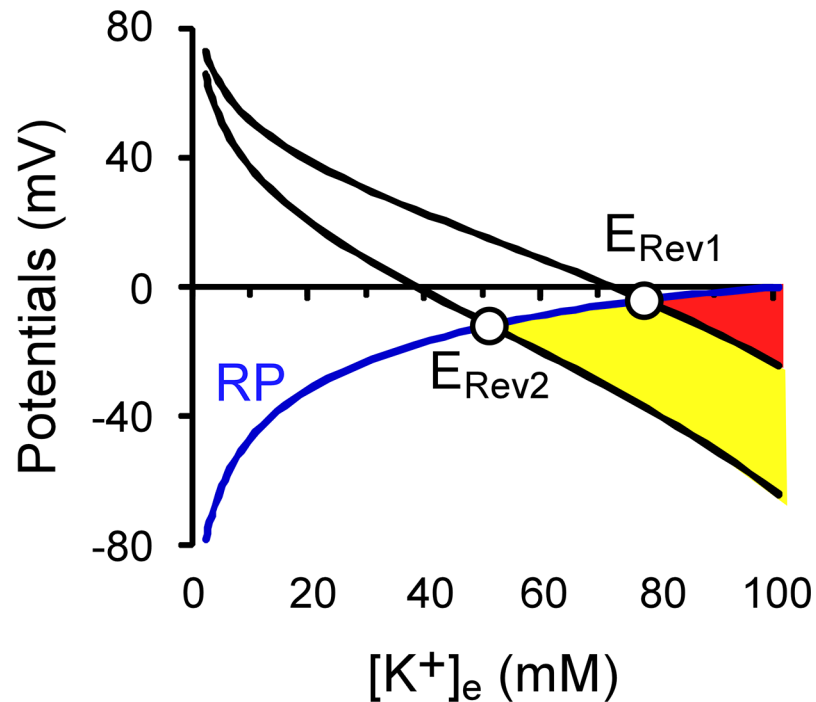
Fig 8. Reversal potential of GLT-1 transport during simulated ischemia depends on GTS. The resting potential (RP) depolarizes when extracellular potassium concentration rises during modeled ischemia. When GLT-1 reversal potential either with only one glutamate molecule transported per cycle (E_{Rev1}), or when the 2nd glutamate molecule is transported per cycle with 50% probability (E_{Rev2}) are more positive than the RP, the transporter operates in normal mode and clears extracellular glutamate. The circles show the conditions of GLT-1 transport reverse at these two different transport stoichiometries.

doi:10.1371/journal.pone.0136111.g008

Acknowledgments

Author Contributions

Conceived and designed the experiments: AYK PAR. Performed the experiments: AYK. Analyzed the data: AYK PAR. Wrote the paper: AYK PAR. Mathematical analysis: AYK.

References

1. Rosenberg PA, Aizenman E (1989) Hundred-fold increase in neuronal vulnerability to glutamate toxicity in astrocyte-poor cultures of rat cerebral cortex. Neuroscience letters 103: 162–168. PMID: 2570387

2. Rosenberg PA, Amin S, Leitner M (1992) Glutamate uptake disguises neurotoxic potency of glutamate agonists in cerebral cortex in dissociated cell culture. J Neurosci 12: 56–61. PMID: 1345946

3. Danbolt NC (2001) Glutamate uptake. Prog Neurobiol 65: 1–105. PMID: 11369436

4. Tanaka K, Watase K, Manabe T, Yamada K, Watanabe M, Takahashi K, et al. (1997) Epilepsy and exacerbation of brain injury in mice lacking the glutamate transporter GLT-1. Science 276: 1699–1702. PMID: 9180080

5. Selkirk JV, Nottebaum LM, Vana AM, Verge GM, Mackay KB, Stiefel TH, et al. (2005) Role of the GLT-1 subtype of glutamate transporter in glutamate homeostasis: the GLT-1-preferring inhibitor WAY-855 produces marginal neurotoxicity in the rat hippocampus. Eur J Neurosci 21: 3217–3228. PMID: 16026460

6. Zerangue N, Kavanaugh MP (1996) Flux coupling in a neuronal glutamate transporter. Nature 383: 634–637. PMID: 8857541

7. Levy LM, Warr O, Attwell D (1998) Stoichiometry of the glial glutamate transporter GLT-1 expressed inducibly in a Chinese hamster ovary cell line selected for low endogenous Na+-dependent glutamate uptake. J Neurosci 18: 9620–9628. PMID: 9822723

8. Owe SG, Marcaggi P, Attwell D (2006) The ionic stoichiometry of the GLAST glutamate transporter in salamander retinal glia. J Physiol 577: 591–599. PMID: 17008380

9. Fairman WA, Vandenberg RJ, Arriza JL, Kavanaugh MP, Amara SG (1995) An excitatory amino-acid transporter with properties of a ligand-gated chloride channel. Nature 375: 599–603. PMID: 7791878

10. Grewer C, Balani P, Weidenfeller C, Bartusel T, Tao Z, Rauen T (2005) Individual subunits of the glutamate transporter EAAC1 homotrimer function independently of each other. Biochemistry 44: 11913–11923. PMID: 16128593

11. Utsunomiya-Tate N, Endou H, Kanai Y (1997) Tissue specific variants of glutamate transporter GLT-1. FEBS Lett 416: 312–316. PMID: 9373176

12. Chen W, Aoki C, Mahadomrongkul V, Gruber CE, Wang GJ, Blitzblau R, et al. (2002) Expression of a variant form of the glutamate transporter GLT1 in neuronal cultures and in neurons and astrocytes in the rat brain. J Neurosci 22: 2142–2152. PMID: 11896154

13. Reye P, Sullivan R, Pow DV (2002) Distribution of two splice variants of the glutamate transporter GLT-1 in the developing rat retina. J Comp Neurol 447: 323–330. PMID: 11992519

14. Chen W, Mahadomrongkul V, Berger UV, Bassan M, DeSilva T, Tanaka K, et al. (2004) The glutamate transporter GLT1a is expressed in excitatory axon terminals of mature hippocampal neurons. J Neurosci 24: 1136–1148. PMID: 14762132

15. Schmitt A, Asan E, Lesch KP, Kugler P (2002) A splice variant of glutamate transporter GLT1/EAAT2 expressed in neurons: cloning and localization in rat nervous system. Neuroscience 109: 45–61. PMID: 11784699

16. Bassan M, Liu H, Madsen KL, Armsen W, Zhou J, Desilva T, et al. (2008) Interaction between the glutamate transporter GLT1b and the synaptic PDZ domain protein PICK1. Eur J Neurosci 27: 66–82. doi: 10.1111/j.1460-9568.2007.05986.x PMID: 18184314

17. Rauen T, Wiessner M, Sullivan R, Lee A, Pow DV (2004) A new GLT1 splice variant: cloning and immunolocalization of GLT1c in the mammalian retina and brain. Neurochem Int 45: 1095–1106. PMID: 15337309

18. Macnab LT, Pow DV (2007) Expression of the exon 9-skipping form of EAAT2 in astrocytes of rats. Neuroscience 150: 705–711. PMID: 17981401

19. Furness DN, Dehnes Y, Akhtar AQ, Rossi DJ, Hamann M, Grutle NJ, et al. (2008) A quantitative assessment of glutamate uptake into hippocampal synaptic terminals and astrocytes: new insights into a neuronal role for excitatory amino acid transporter 2 (EAAT2). Neuroscience 157: 80–94. doi: 10.1016/j.neuroscience.2008.08.043 PMID: 18805467

20. Danbolt NC, Furness DN, Dehnes Y, Qureshi A, Rossi D, Hamann M, et al. (2006) A quantitative assessment of glutamate uptake into hippocampal synaptic terminals and astrocytes. Program No 6298 2006 Abstract Viewer/Itinerary Planner Washington, DC: Society for Neuroscience, 2006 Online.

21. Melone M, Bellesi M, Conti F (2009) Synaptic localization of GLT-1a in the rat somatic sensory cortex. Glia 57: 108–117. doi: 10.1002/glia.20744 PMID: 18720407

22. Herman MA, Jahr CE (2007) Extracellular glutamate concentration in hippocampal slice. J Neurosci 27: 9736–9741. PMID: 17804634

23. Clements JD, Lester RA, Tong G, Jahr CE, Westbrook GL (1992) The time course of glutamate in the synaptic cleft. Science 258: 1498–1501. PMID: 1359647

24. Raghavachari S, Lisman JE (2004) Properties of quantal transmission at CA1 synapses. J Neurophysiol 92: 2456–2467. PMID: 15115789

25. Saftenku EE (2005) Modeling of slow glutamate diffusion and AMPA receptor activation in the cerebellar glomerulus. J Theor Biol 234: 363–382. PMID: 15784271

26. Diamond JS, Jahr CE (2000) Synaptically released glutamate does not overwhelm transporters on hippocampal astrocytes during high-frequency stimulation. Journal of neurophysiology 83: 2835–2843. PMID: 10805681

27. Kabakov AY, Rosenberg PA (2009) Evidence for change in current-flux coupling of GLT1 at high gluta-mate concentrations in rat primary forebrain neurons and GLT1a-expressing COS-7 cells. The Euro-pean journal of neuroscience 30: 186–195. doi: 10.1111/j.1460-9568.2009.06809.x PMID: 19614985

28. DeFelice LJ (2004) Transporter structure and mechanism. Trends Neurosci 27: 352–359. PMID: 15165740

29. Accardi A, Miller C (2004) Secondary active transport mediated by a prokaryotic homologue of ClC Cl-channels. Nature 427: 803–807. PMID: 14985752

30. Sonders MS, Zhu SJ, Zahniser NR, Kavanaugh MP, Amara SG (1997) Multiple ionic conductances of the human dopamine transporter: the actions of dopamine and psychostimulants. J Neurosci 17: 960–974. PMID: 8994051

31. Galli A, Blakely RD, DeFelice LJ (1998) Patch-clamp and amperometric recordings from norepineph-rine transporters: channel activity and voltage-dependent uptake. Proc Natl Acad Sci U S A 95: 13260–13265. PMID: 9789076

32. Petersen CI, DeFelice LJ (1999) Ionic interactions in the Drosophila serotonin transporter identify it as a serotonin channel. Nat Neurosci 2: 605–610. PMID: 10404179

33. Adams SV, DeFelice LJ (2003) Ionic currents in the human serotonin transporter reveal inconsistencies in the alternating access hypothesis. Biophys J 85: 1548–1559. PMID: 12944272

34. Beckman ML, Quick MW (2001) Substrates and temperature differentiate ion flux from serotonin flux in a serotonin transporter. Neuropharmacology 40: 526–535. PMID: 11249962

35. Kang TM, Hilgemann DW (2004) Multiple transport modes of the cardiac Na+/Ca2+ exchanger. Nature 427: 544–548. PMID: 14765196

36. Wadiche JI, Kavanaugh MP (1998) Macroscopic and microscopic properties of a cloned glutamate transporter/chloride channel. J Neurosci 18: 7650–7661. PMID: 9742136

37. Wang GJ, Chung HJ, Schnuer J, Pratt K, Zable AC, Kavanaugh MP, et al. (1998) High affinity glutamate transport in rat cortical neurons in culture. Mol Pharmacol 53: 88–96. PMID: 9443935

38. Gluzman Y (1981) SV40-transformed simian cells support the replication of early SV40 mutants. Cell 23: 175–182. PMID: 6260373

39. Bergles DE, Jahr CE (1998) Glial contribution to glutamate uptake at Schaffer collateral-commissural synapses in the hippocampus. J Neurosci 18: 7709–7716. PMID: 9742141

40. Wadiche JI, Arriza JL, Amara SG, Kavanaugh MP (1995) Kinetics of a human glutamate transporter. Neuron 14: 1019–1027. PMID: 7748550

41. Kabakov AY (1998) Activation of KATP channels by Na/K pump in isolated cardiac myocytes and giant membrane patches. Biophys J 75: 2858–2867. PMID: 9826607

42. Mercik K, Zarnowska ED, Mandat M, Mozrzymas JW (2002) Saturation and self-inhibition of rat hippo-campal GABA(A) receptors at high GABA concentrations. Eur J Neurosci 16: 2253–2259. PMID: 12492419

43. Bergles DE, Tzingounis AV, Jahr CE (2002) Comparison of coupled and uncoupled currents during glu-tamate uptake by GLT-1 transporters. J Neurosci 22: 10153–10162. PMID: 12451116

44. Torres-Salazar D, Fahlke C (2006) Intersubunit interactions in EAAT4 glutamate transporters. J Neu-rosci 26: 7513–7522. PMID: 16837599

45. Kanner BI (2006) Structure and function of sodium-coupled GABA and glutamate transporters. J Membr Biol 213: 89–100. PMID: 17417704

46. Bergles DE, Jahr CE (1997) Synaptic activation of glutamate transporters in hippocampal astrocytes. Neuron 19: 1297–1308. PMID: 9427252

47. Diamond JS, Jahr CE (1997) Transporters buffer synaptically released glutamate on a submillisecond time scale. J Neurosci 17: 4672–4687. PMID: 9169528

48. Grunewald M, Menaker D, Kanner BI (2002) Cysteine-scanning mutagenesis reveals a conformation-ally sensitive reentrant pore-loop in the glutamate transporter GLT-1. J Biol Chem 277: 26074–26080. PMID: 11994293

49. Tong G, Jahr CE (1994) Block of glutamate transporters potentiates postsynaptic excitation. Neuron 13: 1195–1203. PMID: 7946356

50. Potier B, Billard JM, Riviere S, Sinet PM, Denis I, Champeil-Potokar G, et al. (2010) Reduction in gluta-mate uptake is associated with extrasynaptic NMDA and metabotropic glutamate receptor activation at the hippocampal CA1 synapse of aged rats. Aging cell 9: 722–735. doi: 10.1111/j.1474-9726.2010.00593.x PMID: 20569241

51. Sheardown MJ, Nielsen EO, Hansen AJ, Jacobsen P, Honore T (1990) 2,3-Dihydroxy-6-nitro-7-sulfa-moyl-benzo(F)quinoxaline: a neuroprotectant for cerebral ischemia. Science 247: 571–574. PMID: 2154034

52. Follett PL, Rosenberg PA, Volpe JJ, Jensen FE (2000) NBQX attenuates excitotoxic injury in developing white matter. J Neurosci 20: 9235–9241. PMID: 11125001